Acta Neuropathol (1999) 97:577–584

REGULAR PAPER

Hitoshi Kikuchi · Katsumi Doh-ura · Jun-ichi Kira
Toru Iwaki

Preferential neurodegeneration in the cervical spinal cord of progressive supranuclear palsy

Received: 17 August 1998 / Revised, accepted: 9 November 1998

Abstract Spinal cord lesions have seldom been described in cases with progressive supranuclear palsy (PSP). We thus decided to analyze spinal cord lesions by microtubule-associated protein 2 (MAP2) immunohistochemistry in six cases of PSP, five cases of Parkinson's disease (PD) and two cases of corticobasal degeneration (CBD), all of which cause parkinsonism, while six patients without any neurological disease served as controls. In the PSP cases, the MAP2 expression in the cervical spinal cords significantly decreased in the medial division of the anterior gray horn, intermediate gray and posterior gray horn, but showed no significant change in the substantia gelatinosa and lateral division of the anterior gray horn. The thoracic and lumbar spinal cords were well preserved for MAP2 immunoreactivity. In addition, the globose type neurofibrillary tangles and glial fibrillary tangles were more conspicuous in the cervical than in the thoracic and lumbar spinal cord in PSP cases. On the other hand, the PD and CBD cases showed no significant decrease of MAP2 immunoreactivity in the spinal cords. The small neurons, which are located rather selectively in the intermediate zone of the spinal cord, are considered to be mostly present in the interneurons, and are also thought to play a role in various types of focal dystonia, such as neck dystonia. We therefore consider the distinct decrease in the MAP2-positive neuronal processes in the cervical spinal cord may partly reflect the loss of interneurons and may, thereby, possibly cause nuchal dystonia.

H. Kikuchi (✉) · K. Doh-ura · T. Iwaki
Department of Neuropathology, Neurological Institute,
Faculty of Medicine, Kyushu University 60,
Fukuoka 812-8582, Japan
Tel.: +81-92-642-5537, Fax: +81-92-642-5540

H. Kikuchi · J. Kira
Department of Neurology, Neurological Institute,
Faculty of Medicine, Kyushu University,
Fukuoka 812-8582, Japan

Key words Progressive supranuclear palsy · Microtubule-associated protein 2 · Semiquantitative analysis · Spinal cord · Dystonia

Introduction

Progressive supranuclear palsy (PSP) is a disorder characterized by supranuclear ophthalmoplagia, akinesia, rigidity, nuchal dystonia, pseudobulbar palsy and cognitive abnormalities leading to dementia. The neuropathological changes of this disease have been described as neuronal loss and astrocytosis with neurofibrillary tangles (NFT) in the oculomotor nucleus, substantia nigra and basal ganglia [32]. Furthermore, abnormal glial cytoskeletal structures, such as tuft-shaped astrocytes, coiled bodies and argyrophilic threads, were found beyond these lesions [19, 20]. The pathological changes of the spinal cord have so far only been rarely and briefly documented.

Microtubule-associated protein 2 (MAP2) promotes tubulin polymerization into the microtubules, and also regulates microtubule assembly and disassembly. In the central nervous system, MAP2 is a stringent marker confined to neuronal cell bodies and dendrites [35]. We have previously reported the usefulness of MAP2 immunostaining for semiquantitative analysis of spinal cord lesions in amyotrophic lateral sclerosis [14]. We have, therefore, also utilized MAP2 immunohistochemistry to investigate the spinal cord lesions in progressive supranuclear palsy (PSP), Parkinson's disease (PD) and corticobasal degeneration (CBD), all of which cause parkinsonism.

Materials and methods

Tissue source

This investigation was carried out the spinal cords obtained at autopsy from six cases of PSP (average age: 71.7 years old), five cases of PD (average: age 75.2 years old), two cases of CBD (average age: 68 years old) and six control cases (average age: 66.8 years old). The postmortem interval ranged from 3 to 21 h

Table 1 Clinical summary. For control cases causes of death are given (*PSP* progressive supranuclear palsy, *PD* Parkinson's disease, *CBD* corticobasal degeneration)

Case no.	Age (years)	Sex	Duration (years)	Major clinical symptoms
PSP				
1	62	M	3	Severe neck dystonia, limb rigidity, dementia, ataxic gait, gaze palsy
2	75	M	4	Severe neck dystonia, dementia, gaze palsy, pseudobulbar palsy
3	61	M	7	Severe neck dystonia, limb rigidity, dementia, gait disturbance, gaze palsy
4	80	F	7	Severe neck dystonia, limb rigidity, dementia, supranuclear gaze palsy
5	77	F	7	Severe neck dystonia, limb rigidity, dementia, gait disturbance, supranuclear gaze palsy
6	75	F	10	Severe neck dystonia, limb rigidity, supranuclear gaze palsy, mild dementia
PD				
P-1	74	M	3	Gait disturbance, rigidity, dementia
P-2	87	M	7	Bilateral tremor, rigidity, dementia
P-3	67	F	20	Light side tremor, rigidity
P-4	80	M	30	Gait disturbance, limb rigidity
P-5	67	F	33	Right side tremor, rigidity
CBD				
CB-1	67	M	8	Right limb kinetic apraxia, rigidity
CB-2	69	F	8	Right limb apraxia, rigidity, aphasia
Control cases				
C-1	48	M		Chronic renal failure
C-2	61	M		Liver cirrhosis
C-3	62	M		Hepatocellular carcinoma, liver cirrhosis
C-4	71	F		Chronic renal failure, diabetes mellitus
C-5	73	M		Lung cancer
C-6	86	F		Lung cancer

(average: 7 h). The clinical involvements of PSP, PD and CBD are summarized in Table 1. We diagnosed PSP and CBD clinicopathologically according to the NINDS-SPSP and preliminary NINDS diagnostic criteria [18, 19]. PD was diagnosed based on the neuronal degeneration of the nigrostriatal system associated with Lewy bodies.

The spinal cords were fixed for 2 weeks in buffered 10% formalin, and then embedded in paraffin. After embedding, 6-μm-thick sections were prepared. For the routine neuropathological study, the sections were stained with hematoxylin-eosin (H&E), Bodian's stain and Klüver-Barrera (K-B) stain. The number of small neurons was counted by cresyl violet staining, while the presence of gliosis was evaluated by both Holzer staining and glial fibrillary acidic protein (GFAP) immunostaining. The sixth cervical level, fourth thoracic level and third lumbar level of the spinal cord were pathologically evaluated.

Antibodies

The following antibodies were used in the immunohistochemical assays: mouse monoclonal antibodies (mAb) against MAP2 [clone AP-20, Boehringer Mannheim, Germany, 5 μg/ml; clone HM-2, Sigma, 1:500 (HM-2 reacts with all known forms of MAP2, i.e., MAP2a, MAP2b and MAP2c, while AP20 recognizes an epitope on high molecular weight MAP2 forms, such as, MAP2a and MAP2b, but shows no reaction with MAP2c)]; a mouse mAb against phosphorylated neurofilament (clone 2F11, DAKO, 1:500); rabbit antiserum against rat tau (1:1000) [22]; and rabbit antiserum against GFAP (DAKO, 1:1000).

Immunohistochemistry

Immunohistochemical staining was carried out using indirect immunoperoxidase. Peroxidase-conjugated anti-mouse or anti-rabbit IgG were purchased from Vector laboratories (USA). The sections were deparaffinized in xylene, hydrated in ethanol, and incubated with 0.3% hydrogen peroxide in absolute methanol for 30 min at room temperature to inhibit endogenous peroxidase. After rinsing in tap water, the sections were completely immersed in distilled water and were autoclaved at 120 °C for 10 min to enhance the immunoreactivity for MAP2. After pretreatment, the sections were incubated with a primary antibody diluted in TBST (25 mM TRIS-HCl pH 7.6, 0.5 M NaCl, 0.05% NaN_3, 0.05% Tween 20) containing 5% nonfat milk at 4 °C overnight and then with an anti-mouse or anti-rabbit IgG antibody conjugated with horseradish peroxidase (1:200) in phosphate-buffered saline for 30–60 min at room temperature. The colored reaction product was developed with 3,3′-diaminobenzidine tetrahydrochloride (DAB) solution (0.02% DAB, 0.003% H_2O_2, 50 mM TRIS-HCl, pH 7.6). The sections were then counterstained lightly with hematoxylin.

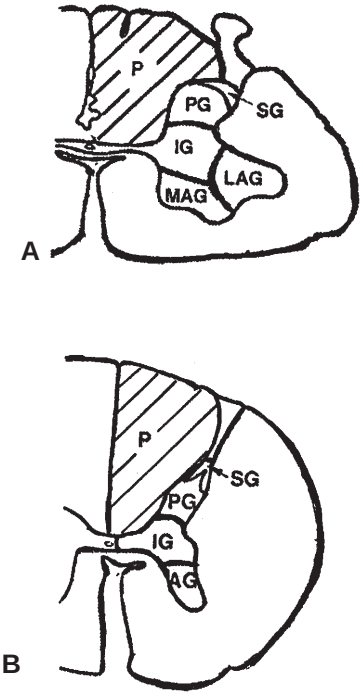

Fig. 1 Schematic drawing of the cervical spinal cord (**A**) and the thoracic spinal cord (**B**) (*SG* substantia gelatinosa, *PG* posterior gray horn, *IG* intermediate gray, *MAG* medial division of the anterior gray horn, *LAG* lateral division of the anterior gray horn, *AG* anterior gray horn, *P* posterior column whose density was used to calibrate the background density)

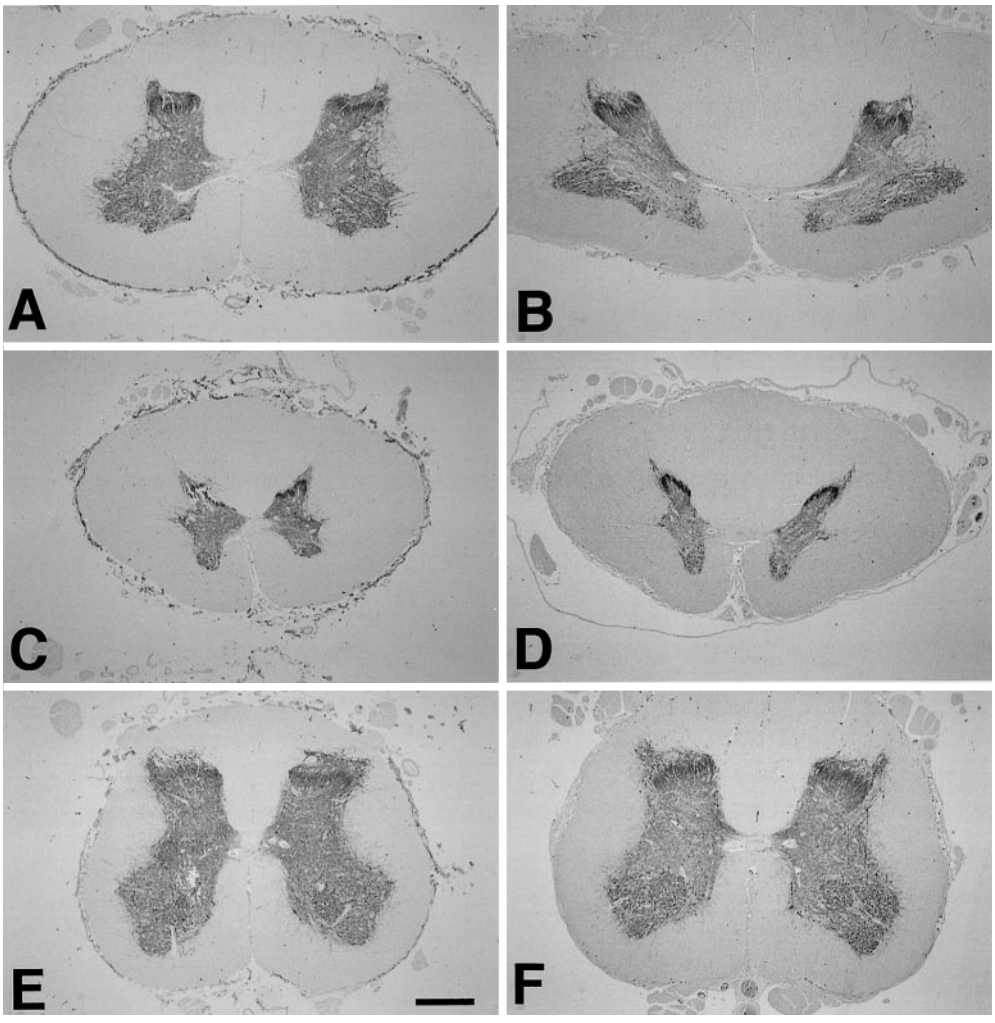

Fig. 2 Comparative immunohistochemistry of the sixth cervical spinal cord (**A, B**), the fourth thoracic spinal cord (**C, D**) and the third lumbar spinal cord (**E, F**) of either the control cases (**A, C, E**) or the PSP cases (**B, D, F**) probed with monoclonal antibody against MAP2. Positive immunoreactivity for MAP2 is well preserved in the gray matter from the control case (**A, C, E**, case C-3). MAP2 immunoreactivity of the PSP case symmetrically decreased more in the medial portion of the anterior gray horn, intermediate gray and posterior gray horn than in the lateral portion and substantia gelatinosa in the cervical spinal cord (case 5; **B**). On the other hand, the MAP2 immunoreactivity of the thoracic and lumbar spinal cord is relatively well preserved in the PSP case (**D, F**) (PSP progressive supranuclear palsy, MAP2 microtubule-associated protein 2). *Bar* **E** (also for **A–D, F**) 1 mm

Semiquantitative analyses

To measure MAP2 immunoreactivity, cross-sections of the spinal cord at the sixth cervical level (C6), the third lumbar level (L3) and fourth thoracic level (T4) were partitioned as shown in Fig. 1 (the lumber area is divided in the same manner as the cervical area). Images of the sections were scanned by Scanjet IIc (Hewlett Packard, USA) and Adobe Photoshop software version 3.0J. A densitometric analysis was performed using NIH image software version 1.60.

The quantity of the MAP2-immunoreactivity products was expressed as the optical density (OD). The relative amount of MAP2 in the posterior gray horn (PG) was calculated as (OD_{PG}–OD_P) divided by (OD_{SG}–OD_P), MAP2 in the intermediate gray (IG) was calculated as (OD_{IG}–OD_P) divided by (OD_{SG}–OD_P), MAP2 in the medial division of the anterior gray horn (MAG) was calculated as (OD_{MAG}–OD_P) divided by (OD_{SG}–OD_P), MAP2 in the lateral division of the anterior gray horn (LAG) was calculated as (OD_{LAG}–OD_P) divided by (OD_{SG}–OD_P), MAP2 in the anterior gray horn (AG) was calculated as (OD_{AG}–OD_P) divided by (OD_{SG}–OD_P), where OD_{PG}, OD_{IG}, OD_{MAG}, OD_{LAG}, OD_{AG}, OD_{SG} and OD_P stand for the average OD per area in the PG area, in the IG area, in the MAG area, in the LAG area, in the AG area, in the substantia gelatinosa (SG) area and in the posterior column (P) area, respectively (Fig. 1).

The data obtained were assessed by Student's *t*-test and Welch's *t*-test. We analyzed the bilateral sides of the cross-sections, and no significant difference was found between the results from either side. Thus, for simplicity, we report the data of the right side of the spinal cord in the results.

Results

Immunohistochemistry using two distinct monoclonal antibodies against MAP2, consisting of clone HM-2 and clone AP20, showed identical results in the cases examined. Thus, we show only the immunohistochemical findings of clone AP20 in the figures.

Controls

The gray matter of the spinal cord displayed diffuse, positive immunostaining for MAP2 (Figs. 2 A, C, E). The white matter was not immunolabeled. The OD patterns of MAP2 are shown in Fig. 4.

PSP cases

No neuronal loss or degeneration in the spinal cords was evident, but fibrillary gliosis was detected in the MAG of the cervical spinal cords in half of the PSP cases (cases 1,

Table 2 Pathology of the spinal cords in PSP cases. For MAP2, values of the relative optical density are given as: *0* > 0.5, *–1* 0.3–0.5, *–2* < 0.3; for NFT, the number per each section are given; for GFT (such as tuft-shaped astrocytes and coiled bodies): *0* none, *+ 1* few, *+ 3* numerous, *+ 2* between +1 and +3; for gliosis: – none, + mild; for axonal swelling: *0* none, *+ 1* few, *+ 3* numerous, *+ 2* between +1 and + 3 (*C-cord* cervical spinal cord, *T-cord* thoracic spinal cord, *L-cord* lumbar spinal cord, *NFT* neurofibrillary tangle, *GFT* glial fibrillary tangles, *PG* posterior gray horn, *IG* intermediate gray, *MAG* medial division of the anterior gray horn, *LAG* lateral division of the anterior gray horn, *AG* anterior gray horn)

	C-cord				T-cord			L-cord			
	PG	IG	MAG	LAG	PG	IG	AG	PG	IG	MAG	LAG
Case 1											
MAP2	–1	–2	–1	0	0	0	0	–1	–2	–1	0
NFT	5	3	0	0	0	0	2	0	3	0	0
GFT	+1	+1	+1	0	0	0	0	0	0	0	0
Gliosis	–	–	+	–	–	–	–	–	–	–	–
Axonal swelling	+1	+1	+2	0	0	0	+2	+1	+1	+1	+1
Case 2											
MAP2	–1	–2	0	0	0	0	0	0	0	0	0
NFT	0	0	0	0	0	1	0	0	0	0	0
GFT	0	0	0	0	0	0	0	0	0	0	0
Gliosis	–	–	–	–	–	–	–	–	–	–	–
Axonal swelling	+1	+1	+2	+1	0	0	+1	+1	+1	+2	+1
Case 3											
MAP2	0	–1	–1	0	–1	–1	–1	0	–1	–1	0
NFT	6	3	4	1	0	3	0	5	5	3	0
GFT	+1	+2	+2	+2	+1	+1	+1	+1	+2	+1	+1
Gliosis	–	–	–	–	–	–	–	–	–	–	–
Axonal swelling	+1	+1	+2	+1	+1	0	+1	0	+1	+3	+1
Case 4											
MAP2	0	0	0	0	0	0	0	0	0	0	0
NFT	0	0	0	0	0	0	0	0	0	0	0
GFT	0	+1	0	0	0	0	0	0	+1	0	0
Gliosis	–	–	–	–	–	–	–	–	–	–	–
Axonal swelling	+1	0	0	+1	0	0	+1	0	0	+2	0
Case 5											
MAP2	–1	–1	–1	0	0	–1	–1	0	0	0	0
NFT	0	1	1	0	0	0	0	0	0	0	0
GFT	+1	+1	0	0	0	0	0	0	0	0	0
Gliosis	–	+	+	–	–	–	–	–	–	–	–
Axonal swelling	+1	+1	+1	+1	0	0	0	0	0	+2	+1
Case 6											
MAP2	–1	–2	–1	0	–1	0	–1	0	0	0	0
NFT	2	2	2	0	0	3	0	1	0	0	0
GFT	0	0	+1	0	0	0	0	0	0	0	0
Gliosis	–	–	+	–	–	–	–	–	–	–	–
Axonal swelling	+1	+1	+1	0	0	0	0	+1	0	+1	0

5, 6; Table 2). In the cervical spinal cords, MAP2 immunoreactivity was preferentially decreased in the MAG, IG and PG, but it was relatively preserved in the LAG and SG (Figs. 2B, 3B). The thoracic and lumbar spinal cords were not affected (Fig. 2D, F).

Cytopathologically, MAP2 immunoreactivity dramatically decreased in the IG in the PSP cases (Fig. 3D), and the number of small neurons in the IG decreased in several PSP cases (cases 1–3, 5, 6; Fig. 3H) compared to the control cases (Fig. 3G). The small neurons in the IG of the cervical spinal cords were also enumerated for each high power field (× 200). In general, the number of small neurons in the PSP cases (range: 6–7, average: 9.2, $n = 6$) was smaller than in the control cases (range: 5–21, average: 14.0, $n = 6$), although the difference was not statistically significant ($P = 0.088$). In the anterior gray horn in the PSP cases, MAP2 immunoreactivity was almost completely preserved in the perikarya of remaining motor neurons, but the neuropil immunostaining preferentially decreased (Fig. 3F) compared to the control cases (Fig. 3E).

When the semiquantitative data on MAP2 immunoreactivity in the PSP cases were compared with the control cases, immunoreactivity in the MAG, IG and PG areas in the cervical spinal cords all significantly decreased in the PSP cases ($P < 0.01$), but no significant difference were observed in any other areas (Fig. 4). The semiquantitative data of the MAP2 in (OD_{SG}–OD_P), showed no significant difference between any of the PSP cases and the control cases (C-cord: $P = 0.35$, T-cord: $P = 0.93$, L-cord: $P = 0.11$).

Immunostaining for tau protein revealed the presence of globose type NFT and glial fibrillary tangles (GFT) as tuft-shaped astrocytes and coiled bodies in the spinal cords of the PSP case (Table 2). NFT and GFT were more

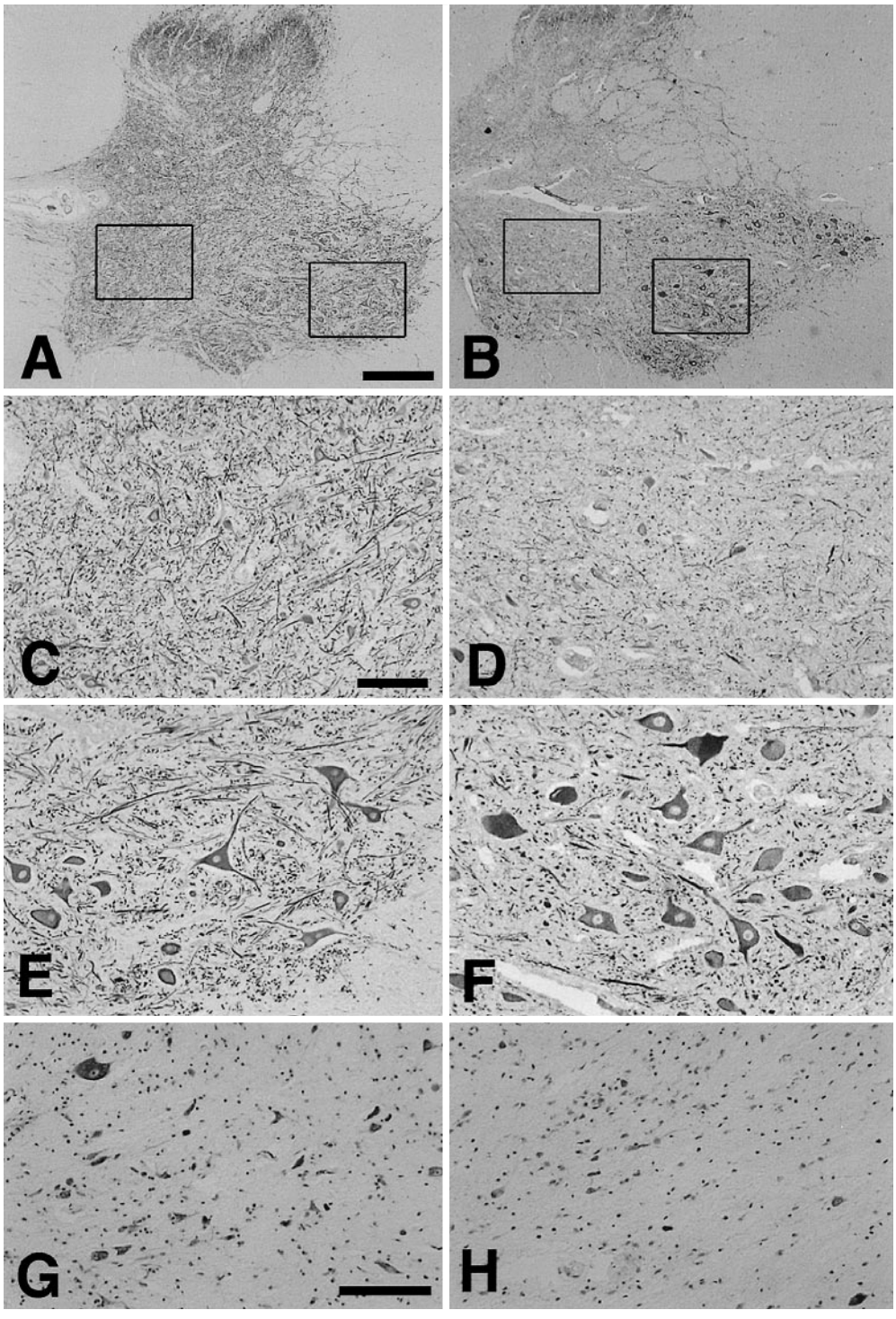

Fig. 3 Neurodegeneration of the cervical spinal cord in the PSP (case 2, **B, D, F, H**) compared with that of the control case (case C-6, **A, C, E, G**). MAP2 immunoreactivity of the intermediate gray and anterior gray horn are well preserved in the control case (**A, C, E**) (**C** and **E** are a magnified view of the *rectangles* in **A**). On the other hand, MAP2 immunoreactivity is decreased predominantly in medial division of intermediate gray (**D**), anterior gray horn (**F**) and posterior gray horn in the PSP case (**B**) (**D** and **F** are magnified view of the *rectangles* in **B**). In the PSP case, the MAP2 immunoreactivity of the intermediate gray is dramatically decreased, especially in the neuropil (**D**), while the MAP2 immunoreactivity of the individual motor neurons is well preserved, but the neuropil immunostaining preferentially decreased in the lateral division of the anterior gray horn (**F**; case 2). The number of small neurons in the intermediate gray decreased significantly more in the PSP case (**H**; case 5) than in the control case (**G**; case C-2). Cresyl violet stain. *Bars* **A** (also for **B**) 700 μm, **C** (also for **D–F**) 100 μm, **G** (also for **H**) 100 μm

conspicuous in the cervical region than in the thoracic and lumbar regions (Table 2).

NF immunoreactivity was enhanced in the axons and the areas of axonal swelling, containing spheroids. Cases 1, 2 and 3 contained numerous scattered axonal swellings in the gray matter of the spinal cord.

Parkinson's disease

The pattern of MAP2 immunoreactivity in the spinal cord was fairly well preserved in the cases of PD. Regarding the semiquantitative data on MAP2 immunoreactivity of the three groups, the control cases, PSP cases and PD cases, no significant difference was seen in the MAP2 immunoreactivity between the control cases and the PD

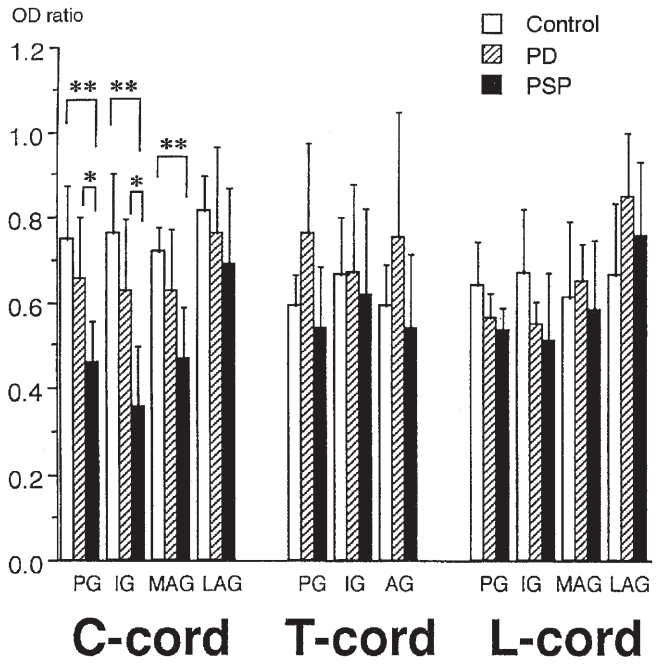

Fig. 4 The relative amount of MAP2 immunoreactivity in the gray matter of the cervical, thoracic and lumbar spinal cords (control $n = 6$, PD $n = 5$, PSP $n = 6$), compared with the controls by Student's *t*-test or Welch's *t*-test. $*P < 0.05$, $**P < 0.01$. MAP2 immunoreactivity of the MAG, IG and PG in the PSP decreased significantly between the control and PSP ($P < 0.01$), and between the PD and PSP ($P < 0.05$), but no significant difference was observed between controls and PD (*PSP* progressive supranuclear palsy, *PD* Parkinson's disease, *PG* posterior gray horn, *IG* intermediate gray, *MAG* medial division of the anterior gray horn, *LAG* lateral division of the anterior gray horn, *AG* anterior gray horn, *C-cord* cervical spinal cord, *T-cord* thoracic spinal cord, *L-cord* lumbar spinal cord)

cases; however, a significant difference between the PD cases and the PSP cases was observed in the cervical spinal cords ($P < 0.05$; Fig. 4).

Corticobasal degeneration

MAP2 immunoreactivity was almost completely preserved in the gray matter of the spinal cords in the two cases of CBD. However, a statistical analysis could not be performed due to the small number of CBD cases. Neither NFT nor GFT were detected in the spinal cord in CBD cases.

Discussion

Our results indicated that PSP showed a degenerative change in the PG, IG and MAG areas of the cervical spinal cord; however, the motor neurons were not necessarily affected. Although the presence of spinal cord lesions in PSP cases is thought to be rare, some previous reports have described the loss of neurons in the anterior horns [5, 6, 12, 16, 27] and the appearance of NFT [4, 34] in the spinal cord of the PSP. Kato et al. [13] investigated the PSP spinal cord in detail, and detected NFT in the anterior horn, lateral horn and posterior horn, especially in the cervical spinal cord, and abnormally thick axons were also observed in the anterior roots. The findings of our current study are in accordance with their findings of spinal cord lesions in PSP cases. The results of a semiquantitative study also demonstrated NFT and GFT to be more conspicuous in the cervical spinal cord, especially in the intermediate zone and PG, than in the thoracic or lumbar spinal cords in the PSP cases.

There are several neurodegenerative diseases, such as PD, CBD and multiple system atrophy, which present with isolated parkinsonism, but other characteristic signs of PSP, such as supranuclear ophthalmoplagia, pseudobulbar palsy, or neck dystonia which appears as an abnormal dorsiflexion of the neck, are not usually found in such diseases [36].

The primary lesions of dystonia in PSP have been considered to be mainly in the basal ganglia and brain stem nuclei [1]. However, dystonia is caused not only by the basal ganglia and brain stem but also by the spinal cord and cerebral cortex [11]. In particular, focal dystonia due to spinal cord lesions has been reported in several diseases [3, 7, 9, 15, 21, 26], and one of the pathophysiological mechanisms of such dystonia cases is considered to be an abnormal excitation of the motor neurons associated with the alteration of the interneurons in the spinal cord. Our study indicates that at least the sixth cervical spinal cord was affected in the PSP case, and the affected area dominates the muscles which regulate both the extension and flexion of the neck [31].

In the spinal cord, the small neurons which are distributed in the intermediate zone of the ventral horn are considered to consist mostly of interneurons [24, 33]. The numerous descending fibers of the extrapyramidal system are mediated by interneurons in the intermediate zone of the cervical spinal cord, such as the rubrospinal tract arising from the cells of the dorsal and dorsomedial parts of the red nucleus (to Rexed V, VI, VII), pontine reticulospinal tract from nuclei reticularis pontis caudalis and oris (to Rexed VII, VIII), and the medullary reticulospinal tract from nucleus reticularis gigantocellularis (to Rexed VII, IX) [23]. These brain stem nuclei are commonly affected in PSP and this was also true in our PSP cases (data not shown). In our study, the MAP2 immunoreactivity in the PSP cases significantly decreased in the areas in which the interneurons existed, and the number of small neurons also decreased in several PSP cases. We thus postulate that a part of the neck rigidity or dystonia, such as abnormal dorsiflexion of the neck, may be caused by either the primary or secondary degeneration of the interneurons of the cervical spinal cord in PSP.

In addition, we also tried to investigate the function of the interneurons using rabbit antiserum against glutamate decarboxylase (GAD) (Chemicon: AB108, 1 : 1000) and mouse mAb anti-parvalbumin (Sigma: clone PA-235, 1 : 1000). GAD is the synthetic enzyme of gamma-aminobutyric acid and parvalbumin is a calcium-binding protein, and both are thought to be markers of interneurons

[8, 29]. However, we failed to evaluate the function of the interneurons, because the immunoreactivities of these two epitopes were inconsistent in our formalin-fixed, paraffin-embedded materials.

CBD as a clinicopathological entity has been described by numerous authors [10, 17, 20, 28, 30]. However, few spinal cord lesions have so far been described. Several authors have described the overlapping clinical features and neuropathological abnormalities between CBD and PSP [2, 25, 37]. It is noteworthy that our present study could not clearly detect CBD spinal cord lesions by MAP2 immunohistochemistry, which may indicate a crucial difference between CBD and PSP. Further investigation is thus needed based on a larger number of CBD cases.

In conclusion, we consider cervical spinal cord lesions to be present in PSP based on the findings of MAP2 immunohistochemistry. The affected areas included the MAG, IG and PG. Interneurons are mostly located in the intermediate zone of the spinal cord, and are thought to participate in various types of focal dystonia, such as neck dystonia. We therefore believe that these lesions may be the cause of nuchal dystonia in PSP.

Acknowledgements The authors thank Ms. K. Hatanaka and Mr. M. Yoneda for their excellent technical assistance and Dr. B. Quinn for comments on the manuscript. We also thank Dr. K. Akazawa, Department of Medical Informatics of Kyushu University Hospital, for his advice on the statistical analyses. This work was supported by the Nakabayashi trust for ALS research (T.I.).

References

1. Agid Y, Javoy-Agid F, Ruberg M, Pillon B, Dubois B, DuycKaerts H, Hauw J-J, Baron J-C, Scatton B (1986) Progressive supranuclear palsy: anatomoclinical and biochemical considerations. Adv Neurol 45:191–206
2. Akashi T, Arima K, Maruyama N, Ando S, Inose T (1989) Severe cerebral atrophy in progressive supranuclear palsy: a case report. Clin Neuropathol 8:195–199
3. Berardelli A, Thompson PD, Day BL, Rothwell JC, O'Brien MD, Marsden CD (1986) Dystonia of the legs induced by walking or passive movement of the big toe in a patient with cerebellar ectopia and syringomyelia. Neurology 36:40–44
4. Behrman S, Carroll JD, Janota I, Matthews WB (1969) Progressive supranuclear palsy: clinico-pathological study of four cases. Brain 92:663–678
5. Blumenthal H, Miller C (1969) Motor nuclear involvement in progressive supranuclear palsy. Arch Neurol 20:362–367
6. Bugiani O, Mancardi GL, Brusa A, Ederli A (1969) The fine structure of subcortical neurofibrillary tangles in progressive supranuclear palsy. Acta Neuropathol 45:147–152
7. Cammarota A, Gershanik OS, García S, Lera G (1995) Cervical dystonia due to spinal cord ependymoma: involvement of cervical cord segments in the pathogenesis of dystonia. Mov Disord 10:500–503
8. Celio MR (1990) Calbindin D-28 k and parvalbumin in the rat nervous system. Neuroscience 35:375–475
9. Cosentino C, Torres L, Flores M, Cuba JM (1996) Paroxysmal kinesigenic dystonia and spinal cord lesion. Mov Disord 11:453–455
10. Gibbs WR, Luthert PJ, Marsden CD (1989) Corticobasal degeneration. Brain 112:1171–1192
11. Hedreen J, Zweig RM, DeLong MR, Whitehouse PJ, Price DL (1988) Primary dystonias: a review of the pathology and suggestions for new directions of study. Adv Neurol 50:123–132
12. Ishino H, Higashi H, Kuroda S, Yabuki S, Hayahara T, Otsuki S (1974) Motor nuclear involvement in progressive supranuclear palsy. J Neurol Sci 22:235–244
13. Kato T, Hirano A, Weinberg MN, Jacobs AK (1986) Spinal cord lesions in progressive supranuclear palsy: some new observations. Acta Neuropathol 71:11–14
14. Kikuchi H, Doh-ura K, Kawashima T, Kira J, Iwaki T (1999) Immunohistochemical analysis of spinal cord lesions in amyotrophic lateral sclerosis using microtubule associated protein 2 (MAP2) antibodies. Acta Neuropathol 97:13–21
15. Kiwak KJ, Deray MJ, Shields WD (1983) Torticollis in three children with syringomyelia and spinal cord tumor. Neurology 33:946–948
16. Kurihara T, Landau WM, Torack RM (1974) Progressive supranuclear palsy with action myoclonus, seizures. Neurology 24:219–223
17. Lippa CF, Smith TW, Fontneau N (1990) Corticonigral degeneration with neuronal achromasia: a clinicopathologic study of two cases. J Neurol Sci 98:301–310
18. Litvan I, Agid Y, Calne D, Campbell G, Dubois B, Duvoisin RC, Goetz CG, Golbe LI, Grafman J, Growdon JH, Hallett M, Jankovic J, Quinn NP, Tolosa E, Zee DS (1996) Cinical research criteria for the diagnosis of progressive supranuclear palsy (Steele-Richardson-Olszewski syndrome): report of the NINDS-SPSP international workshop. Neurology 47:1–9
19. Litvan I, Hauw JJ, Bartko JJ, Lantos PL, Daniel SE, Horoupian DS, McKee A, Dickson D, Bancher C, Tabaton M, Jellinger K, Anderson DW (1996) Validity and reliability of the preliminary NINDS neuropathologic criteria for progressive supranuclear palsy and related disorders. J Neuropathol Exp Neurol 55:97–105
20. Lowe J, Lennox G, Leigh PN (1997) Disorders of movement and system degenerations. In: Graham DI, Lantos PL (eds) Greenfield's neuropathology, 6th edn. Oxford University Press, New York, pp 281–366
21. McKnight P, Friedman J (1992) Torticollis due to cervical epidural abscess and osteomyelitis. Neurology 42:696–697
22. Miyazono M, Iwaki T, Kitamoto T, Shin RW, Fukui M, Tateishi J (1994) Widespread distribution of tau in the astrocytic elements of glial tumors. Acta Neuropathol 86:236–241
23. Parent A (1996) Spinal cord: fiber tracts. Carpenter's human anatomy, 9th edn. Williams and Wilkins, Baltimore, pp 368–417
24. Parent A (1996) Spinal cord: regional anatomy and internal structure. Carpenter's human anatomy, 9th edn. Williams and Wilkins, Baltimore, pp 325–367
25. Paulus W, Selim M (1990) Corticonigral degeneration with neuronal achromasia and basal neurofibrillary tangles. Acta Neuropathol 81:89–94
26. Penry CJK, Hoefnagel D, Noory SVD, Denny-Brown D (1960) Muscle spasm and abnormal postures resulting from damage to interneurones in spinal cord. Arch Neurol 5:500–512
27. Powell HC, London GW, Lampert PW (1974) Neurofibrillary tangles in progressive supranuclear palsy: electron microscopic observations. J Neuropathol Exp Neurol 33:98–106
28. Rebeiz JJ, Kolodny EH, Richardson EP (1968) Corticodentatonigral degeneration with neuronal achromasia. Arch Neurol 18:20–33
29. Ribak CE (1978) Aspinous and sparsely-spinous stellete neurons in the visual cortex of rats contain glutamic acid decarboxylase. J Neurocytol 7:461–478
30. Riley DE, Lang AE, Lewis A, Resch L, Ashby P, Hornykiewicz O, Black S (1990) Cortical-basal ganglionic degeneration. Neurology 40:1203–1212
31. Salmons S (1996) Muscle. In: Williams PL (ed) Gray's anatomy, 13th edn. Churchill Livingstone, New York, pp 737–900

32. Steel J, Richardson J, Olszewski J (1964) Progressive supranuclear palsy: a heterogeneous degeneration involving the brain stem, basal ganglia, and cerebellum with vertical gaze and pseudobulbar palsy, nuchal dystonia and dementia. Arch Neurol 2 : 473–486
33. Terao S, Sobue G, Hashizume Y, Li M, Inagaki T, Mitsuma T (1996) Age-related changes in human spinal ventral horn cells with special reference to the loss of small neurons in the intermediate zone: a quantitative analysis. Acta Neuropathol 92 : 109–114
34. Tomonaga M (1977) Ultrastructure of neurofibrillary tangles in progressive supranuclear palsy. Acta Neuropathol (Berl) 37 : 177–181
35. Tucker RP (1990) The role of microtubule-associated proteins in brain morphogenesis. Brain Res Rev 15 : 101–120
36. Valldeoriola F, Tolosa E, Valls-Solé J (1996) Differential diagnosis and clinical diagnostic criteria of progressive supranuclear palsy. Adv Neurol 69 : 405–412
37. Wakabayashi K, Oyanagi K, Makifuchi T, Ikuta F, Homma A, Homma Y, Horikawa Y, Tokiguchi S (1994) Corticobasal degeneration: etiopathological significance of the cytoskeletal alterations. Acta Neuropathol 87 : 545–553